Ann. Geophys., 26, 3677–3692, 2008
www.ann-geophys.net/26/3677/2008/

Annales Geophysicae

Seasonal, annual and inter-annual features of turbulence parameters over the tropical station Pune (18°32′ N, 73°51′ E) observed with UHF wind profiler

Narendra Singh[1,3], **R. R. Joshi**[2], **H.-Y. Chun**[3], **G. B. Pant**[2], **S. H. Damle**[2], **and R. D. Vashishtha**[4]

[1]Aryabhatta Research Institute of Observational Sciences (ARIES) Manora Peak, Nainital, Uttaranchal, 263129, India
[2]Indian Institute of Tropical Meteorology, Homi Bhabha Road, Pashan, Pune, 411008, India
[3]Department of Atmospheric Sciences, Yonsei University, Seoul, 120749, Korea
[4]India Meteorological Department, Shivaji Nagar, Pune, 411005, India

Received: 11 October 2007 – Revised: 26 August 2008 – Accepted: 13 October 2008 – Published: 24 November 2008

Abstract. The present study is specifically focused on the seasonal, annual and inter-annual variations of the refractive index structure parameter (C_n^2) using three years of radar observations. Energy dissipation rates (ε) during different seasons for a particular year are also computed over a tropical station, Pune. Doppler spectral width measurements made by the Wind Profiler, under various atmospheric conditions, are utilized to estimate the turbulence parameters. The refractive index structure parameter varies from $10^{-17.5}$ to $10^{-13}\,m^{-2/3}$ under clear air to precipitation conditions in the height region of 1.05 to 10.35 km. During the monsoon months, observed C_n^2 values are up to 1–2 orders of magnitude higher than those during pre-monsoon and post-monsoon seasons. Spectral width correction for various non-turbulent spectral broadenings such as beam broadening and shear broadening are made in the observed spectral width for reliable estimation of ε under non-precipitating conditions. It is found that in the lower tropospheric height region, values of ε are in the range of 10^{-6} to $10^{-3}\,m^2\,s^{-3}$. In summer and monsoon seasons the observed values of ε are larger than those in post-monsoon and winter seasons in the lower troposphere. A comparison of C_n^2 observed with the wind profiler and that estimated using Radio Sonde/Radio Wind (RS/RW) data of nearby Met station Chikalthana has been made for the month of July 2003.

Keywords. Meteorology and atmospheric dynamics (Climatology; Convective processes; Tropical meteorology; Turbulence)

Correspondence to: Narendra Singh
(narendra@aries.ernet.in)

1 Introduction

The lower troposphere plays a vital role in various atmospheric processes such as convection triggering, turbulent transport of various quantities like latent heat, pollutants, momentum etc. Knowledge of the turbulence and other atmospheric parameters is essential for several applications in numerical weather prediction, chemical modeling of the atmosphere and in thorough understanding of the dynamics of the lower troposphere. Frictional forces due to earth's orography play a dominant role in generation of turbulence. Turbulent dissipation and diffusion are the processes through which transport of heat, energy, momentum and mass take place in the atmosphere close to the surface of the earth. This can affect the energy budget. Turbulence also influences the diffusion of pollutants from near earth surface to higher altitudes. So, the knowledge of turbulence parameters is essential. Turbulence generated by solar heating of the earth's surface (convection), is known as thermal turbulence and presence of an enhanced wind shear also leads to turbulence, usually called mechanical turbulence which can be frequently seen at the top of the boundary layer. Thermal and mechanical turbulence frequently occur in the lower troposphere.

Observations taken by aircrafts, radiosonde and towers have provided a wealth of information for lower atmospheric studies. However, the development of wind profilers has revolutionized the lower atmospheric studies with their excellent height and temporal resolutions (Gage and Balsley, 1978; Balsley and Gage, 1982). The UHF wind profilers are better suited for lower tropospheric observations (Ecklund et al., 1988; Rogers et al., 1993; Gage et al., 1994; Ralph et al., 1995; Williams et al., 1995; Gossard et al., 1998). One

Published by Copernicus Publications on behalf of the European Geosciences Union.

such UHF radar is located at India Meteorological Department (IMD) Pune (Pant et al., 2005), which is being utilized to carry out studies of turbulence and precipitation. Many researchers have examined the possibility of deducing turbulence parameters viz., refractive index structure parameter (C_n^2), turbulent energy dissipation rate (ε) and eddy diffusivity (K_h) from the observed Doppler spectrum using wind profiling radars (Frisch and Clifford, 1974; Hocking, 1983, 1996; Gage, 1990; Jain et al., 1995; Gossard et al., 1998; White et al., 1999; Ghosh et al., 2001; Satheesan and Krishna Murthy, 2002; Zink et al., 2004).

The 404 MHz profiler detects the clear air and precipitation signal simultaneously, under moderate rain conditions. Since a UHF radar is quite sensitive to hydrometeors it is therefore, during heavy rain, difficult to separate clear air and hydrometeor echoes from the observed Doppler spectrum as the precipitation echoes completely overwhelm the clear air echoes. Clear air signals can be separated from precipitation signals when two peaks are distinct in the spectrum, but this is a rather complex process. It is therefore essential to choose clear days for estimating the energy dissipation rates from the UHF radar observations including the monsoon season.

C_n^2 and ε have previously been estimated over the Indian region by other scientists with radars operating at different frequencies or with RS/RW data (Sarkar et al., 1985; Satheesan and Krishna Murthy, 2002). For the first time, an attempt has been made for this tropical station, to estimate C_n^2 and ε with the wind profiler operating at 404 MHz. The data used for this study is presented in the subsequent section and is intended to examine seasonal, annual and inter-annual variations of C_n^2 and the seasonal variation of ε. The purpose of this study is to add into the observations made by profilers in the tropics and to investigate the significant variability observed in the turbulence. In Sect. 2, systematical account of the data and mathematical formulations used for computing the C_n^2 and ε is given. Section 3 discusses the results and Sect. 4 contains the summary, comments and the concluding remarks.

2 Data base and methods of analysis

Three years of Wind Profiler/Radio Acoustic Sounding System (WP/RASS) observations from June 2003–May 2006, taken on GMT hours at the intervals of 3 h, under various atmospheric conditions, have been utilized. The wind profiler has got two modes of operation, namely lower mode or lower height (LH) and higher mode or higher height (HH). The lower mode of operation starts measurements at range gate 1.05 to 4.35 km and higher mode at 3.15 to 10.35 km. There are 12 range gates in LH and 25 range gates in HH at the equal spacing of 300 m. To study the seasonal, annual and inter-annual features of C_n^2, the data obtained only during the day time observations (i.e. at 03:00, 06:00, 09:00 and 12:00 GMT) for all three years, have been used. Maximum of four observations available during the day time are averaged to get daily means and then further averaged to obtain monthly means. In the case of seasonal variations, only 12:00 GMT data has been utilized. Therefore, to get the seasonal features of the turbulence parameter, this monthly mean profile for different seasons is plotted against altitude to obtain the mean picture of the height profile of C_n^2. In monsoon, June–September, in post-monsoon, October–December, in winter, January–February, and in pre-monsoon or summer, March–May months are taken to analyze the seasonal features. Also standard deviation is calculated with 30 days time series for each month.

The annual variability during the three year period is obtained from monthly mean height profiles of C_n^2 using daily averaged profiler data. The mean inter-annual picture is also examined using the same statistics as in the case of annual variability.

2.1 Formulation for refractive index structure parameter (C_n^2) from wind profiler at Pune

Small scale turbulence plays a crucial role in the atmospheric dynamics, because it not only heats the atmosphere but also causes diffusion of momentum, heat and mass. Since wind profiling radars operating at VHF-UHF bands are mainly sensitive to inhomogeneties in the radio refractive index associated with small scale atmospheric turbulence, the backscattered signal can be effectively used to quantify the effect of turbulence. Atmospheric turbulence is defined by the two parameters refractive index structure constant (C_n^2) and energy dissipation rate (ε).

The magnitude of the backscattered echo from the clear atmosphere depends on the intensity of the refractive index fluctuation/turbulence, which is parameterized by C_n^2. Based on the detectability $(\mathrm{SNR})_{dt}$ given by Gossard and Strauch (1983), we can estimate C_n^2 values at different heights in the atmosphere from the corresponding return signal spectrum. By taking into consideration the coding gain "m" which is 1 for lower mode and 8 for higher mode operation of the wind profiler because at higher altitudes the 16 μs pulse is coded with 8 bauds of 2 μs each. Hence C_n^2 is calculated by knowing the radar parameters (Table 1) as

$$C_n^2 = \frac{5.263m.K_B T_{Op} R^2.\sigma_V (\mathrm{SNR})_{dt}}{K(\alpha_r \alpha_t \overline{P_t} A_e)\lambda^{1/6} \Delta R} \sqrt{\frac{\pi}{T_0 \Delta V}} \quad , \qquad (1)$$

where, K_B = Boltzman constant, σ_v^2 = variance of the signal spectrum, ΔV = spectral measurement resolution (m/s), K = constant which depends on Radar beam width; assuming a Gaussian beam, the constant is 0.0354 (Gossard and Strauch, 1983).

The velocity resolution depends upon the entire Nyquist (unambiguous $V_{\max}=\lambda/4\mathrm{N}_c\mathrm{IPP}$) window of the spectrum, therefore ΔV will be different for Lower and Higher mode operations of the Pune profiler; for lower height

Table 1. Experimental specifications and data processing parameters.

Wind profiler location at Pune (18.5° E, 73.85° N)	
Parameter	Specifications
Radar wave length (λ)	74 cm
Transmitted peak power (P_t)	16 K Watts
Effective aperture (A_e)	80 m^2
3 dB beam width (θ)	$\leq 5°$
Half power beam width of the profiler antenna (θ_p)	2.5°
Off zenith angle or Elevation (χ)	16.3° or 73.7°
Receiver path loss (α_r)	2.2 dB
Transmitter path loss (α_t)	0.8 dB
Kolmogorov Constant (α)	1.6
Total system temperature (T_{op})	800 K
Pulse width (τ) (LH/HH)	2 μs uncoded)/16 μs (8 bit coded of 2 μs baud length)
Inter Pulse Period (IPP) LH/HH	60 μs/160 μs
Range resolution (ΔR)	300 m
Coherent integrations	76 (selectable)
Incoherent integrations	10
Power aperture product	$\sim 2\times 104$ in Lower Mode
(Including losses)	$\sim 7\times 104$ in Higher Mode
Range bins (R) Lower mode, Higher mode	1.05–4.35 (km), 3.15–10.35 (km)
Beam dwell time in sec. (T_0), LH & HH	32.3 & 85.5
3.15–4.35 range bins are common to both modes	

ΔV=0.15 m/s and for higher heights it is 0.06 m/s. The spectral processing gain (SPG) will be different for the two operating modes and C_n^2 is therefore calculated separately for the lower and higher altitudes.

2.2 C_n^2 from Radiosonde/Radiowind (RS/RW)

It is a well established fact that turbulence in the free atmosphere is confined to thin horizontal layers separated by non turbulent regions (Van Zandt et al., 1978; Doviac and Zernic, 1993). Although turbulence in these layers may be inherently inhomogeneous and non isotropic, on local scales much smaller than the thickness of these layers, it can be considered as homogeneous and isotropic. If one further assumes that the time to develop turbulence in the air is much smaller than the overall characteristic time for evolution of the layer, the assumption of a steady state condition for the turbulence may be justified. This is the basic premise of the theory of turbulent structure as enunciated by Tatarskii (1971), who shows that the turbulence structure constant (C_n^2) for the radio refractivity can be written as

$$C_n^2 = a^2 \alpha' l_0^{4/3} M^2 \quad , \tag{2}$$

where, a^2 = constant = 2.8, α' = ratio of eddy diffusivities $\sim$1, l_o = buoyancy/outer scale length of the turbulence spectrum and M = vertical gradient of the potential refractive index fluctuations.

The total turbulent energy density spectrum consists of a production region, the inertial subrange and the dissipation region. Most of the turbulent energy production occurs at scale sizes between $6\,l_o$ and $l_o/6$, where l_o is defined as the generic buoyancy/outer scale of turbulence and $l_o/6$ is defined as the onset of the inertial subrange. The outer scale l_o is presumed to be around 10 m (Van Zandt et al., 1978), although no direct evidence is available on the thickness of a turbulent layer. The value of M is given by the relation (Doviak and Zrnic, 1993),

$$M = -77.6 \times 10^{-6} \left(\frac{P}{T}\right) \left(\frac{\partial \ln \theta_T}{\partial z}\right) \left[1 + \frac{15\,500\,q}{T}\left(1 - \frac{1}{2}\frac{\partial \ln q/\partial z}{\partial \ln \theta_T/\partial z}\right)\right] \quad , \tag{3}$$

where P = atmospheric pressure in mb, T = absolute temperature (K), θ_T = potential temperature (K), q = specific humidity (gm/kg), and z = altitude in meters (m).

It may be noted that value of M can be obtained from the RS/RW measurements of temperature, humidity and pressure for different heights in the atmosphere. One may then estimate the vertical profile of average $\overline{C_n^2}$ from the RS/RW data. However, it is already mentioned that the turbulent layers are rather thin ($l_o \sim$10–20 m) separated by non-turbulent regions and hence in dealing with a radar situation one has to be able to estimate an average fraction of the radar beam/volume which is turbulent, to get the correct estimate of C_n^2. One may therefore, write

$$\overline{C^2_{n(\mathrm{radar})}} = \overline{C_n^2} F \quad , \tag{4}$$

here, "F" is the average fraction of the radar volume which is turbulent. This F factor is calculated from the Van Zandt et al. (1978)'s model.

Calculations based on typical RS/RW data show that F varies from 0.1 to 0.01 in the troposphere for height intervals around 600 m to 1 km. In practice, $\overline{C_{n\,(\mathrm{radar})}^2}$ varies with time of the day by as much as one order of magnitude at a given height. The value of M^2 (and hence $\overline{C_{n\,(\mathrm{radar})}^2}$) is dominated by humidity and its gradient in the lower troposphere. In a dry atmosphere where the humidity (q) is very low beyond a few km altitude, $C_{n\,(\mathrm{radar})}^2$ can be quite low, leading to very weak radar signals even when turbulence may be considerable but the potential temperature gradient may be very low. This limits the height coverage for measurements by the profiler radar in the lower troposphere.

2.3 Estimation of energy dissipation rates (ε)

Turbulent kinetic energy dissipation rate is one of the key parameters in the atmospheric turbulence theory. It represents the rate of transfer of energy from larger to smaller eddies in the inertial subrange of inhomogeneties and rate of conversion of kinetic energy of turbulence into heat in the viscous subrange. Above the boundary layer, the dissipation rate decreases rapidly to low values and rises again in the vicinity of the jet stream (Joshi et al., 2006). The estimation of ε is based on equations that follow from Kolmogorov-Obukhov laws of transformation of turbulent energy. There are three methods proposed in the literature for the estimation of ε from radar measurements. All these methods assume that turbulence is isotropic and well within the inertial subrange. It is also assumed that the spectrum follows a Kolmogorov shape and that the atmosphere is stably stratified. The first two methods are described briefly and the spectral width method, which has been followed in this study, will be discussed in details in the subsequent paragraphs.

2.3.1 Radar backscatter signal power method

The method proposed by Hocking (1983, 1985) uses the 0-th moment of the velocity spectra. It makes use of the measured profile of C_n^2 and requires a well calibrated radar as well as additional information about atmospheric humidity and stability. The method requires a reasonably well calibrated profiler radar system and it also needs auxiliary measurements of humidity and temperature gradients obtained usually by radiosonde balloons, which are not currently available at Pune. In the absence of the availability of such auxiliary data, the spectral width method for estimation of ε is normally the preferred one.

2.3.2 Wind variance method

In this method, wind variance is estimated from spectral analysis of the time series of vertical wind data and the data length must be long enough to fully include the Brunt-Vaisala period. It is generally assumed that the inertial subrange extends up to the buoyancy scale or B-V frequency (Weinstock, 1978), although direct numerical simulation of turbulent flows indicates that the onset of the inertial subrange probably occurs at around $l_B/6$, where l_B is the buoyancy scale of turbulence (Bakker, 2002). Following this, the variance of the vertical wind ($\overline{w^2}$) due to turbulence is obtained by integrating the power spectrum of the vertical wind from the B-V to the Nyquist frequency. This estimate of $\overline{w^2}$ (due to turbulence) could be an underestimate because contributions from frequencies greater than the Nyquist frequency are not considered.

2.3.3 Doppler spectral width method

Since the two methods described above involve various assumptions and approximations, and additional information about the temperature, pressure and humidity parameters are necessary, we therefore use the spectral width method and consider this to be the most suitable method to make correct estimations of energy dissipation rates. The method is precisely discussed in relation to the data archived from the wind profiling radar at Pune. The experimentally observed radial beam spectra are first manually edited to eliminate those spectra, particularly in the lowest two or three range bins, which may be contaminated by interference.

The observed six-minute spectral width (second moment) values for the edited radial beam spectra are corrected for non-turbulent effects. The true turbulence varianceσ_w^2, for the zenith beam, is written as

$$\sigma_w^2 = \sigma_{w(\mathrm{observed})}^2 - \sigma_a^2 \quad , \tag{5}$$

where, σ_a^2 is the correction for the finite beam width and wind shear effect. It is estimated by using Nastrom's (1997) formulation given below:

$$\begin{aligned}\sigma_a^2 = {} & \frac{\theta_p^2}{3} V_T^2 \cos^2\chi - \frac{2\theta_p^2}{3}\left\{\sin^2\chi\right\}\left(V_T \frac{\partial V_T}{\partial Z} r\cos\chi\right) \\ & + \frac{\theta_p^2}{24}\{3+\cos 4\chi - 4\cos 2\chi\}\left(\frac{\partial V_T}{\partial Z}\right)^2 R^2 \\ & + \left\{\frac{\theta_p^2}{3}\cos 4\chi + \sin^2\chi\cos^2\chi\right\}\left(\frac{\partial V_T}{\partial Z}\right)^2 \frac{\Delta R^2}{12}, \end{aligned} \tag{6}$$

where, V_T = average horizontal velocity and $\frac{\partial V_T}{\partial Z}$ = vertical shear of the average horizontal wind. Other variables are given in Table 1. The shear $\frac{\partial V_T}{\partial Z}$ is calculated from the average V_T values for different heights. The corrected σ_w^2 values

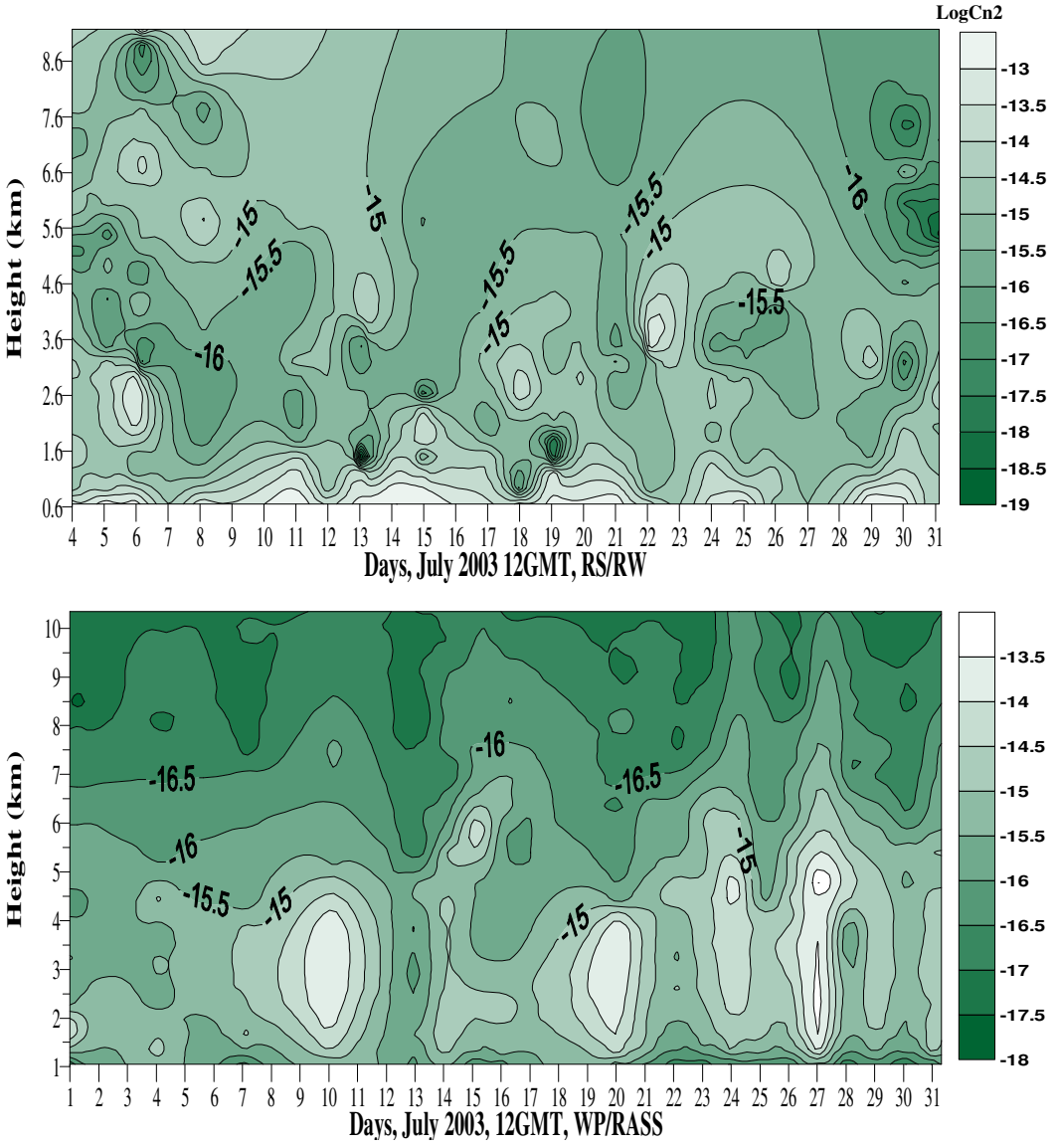

Fig. 1. Height profile of C_n^2 as calculated from RS/RW (upper panel) and wind profiler Observations (lower panel). The radiosonde observations start at few meters (0.6 km) above the ground and wind profiler observations at 1.05 km onwards, the contours above 1 km are to be taken for comparison.

are then averaged to obtain the hourly averaged values of σ_w^2. Hence, ε is calculated by

$$\varepsilon = \frac{1}{\delta}\left[\frac{\sigma_w^2}{\alpha\left\{\frac{3}{2}\Gamma\left(\frac{5}{3}\right)\gamma^2 + \frac{3}{2}\frac{\alpha_1}{\alpha}\left(\frac{2a}{\pi\delta}\right)^{\frac{2}{3}}\left[\left(\frac{V_T T_0}{2a}\right)^{\frac{2}{3}} - 1\right]\right\}}\right]^{\frac{3}{2}}, \quad (7)$$

where, σ_w^2 is the variance in the vertical beam (w) within the pulse volume. The parameters used in Eq. (7) are given by

$$\left.\begin{array}{l}\delta = a = \frac{R\theta}{2} \\ \gamma^2 = 1 - \frac{h}{15} - \frac{h^2}{105} - \ldots\ldots \\ h = 1 - \left(\frac{b}{a}\right)^2\end{array}\right\} \text{ for } b \le a \text{ and}$$

$$\left.\begin{array}{l}\delta = b \equiv \left(\frac{c\tau}{2}\right) \\ \gamma^2 = 1 - \frac{4h}{15} - \frac{8h^2}{105} - \ldots\ldots \\ h = 1 - \left(\frac{a}{b}\right)^2\end{array}\right\} \text{ for } b > a, \quad (8)$$

where c = velocity of light, a = half the diameter of the circular beam cross section, b = half length of the pulse, R = range in meters, γ^2 = confluent hypergeometric expansion introduced by Labbitt for the Frisch integral and α_1 = constant ∼0.5.

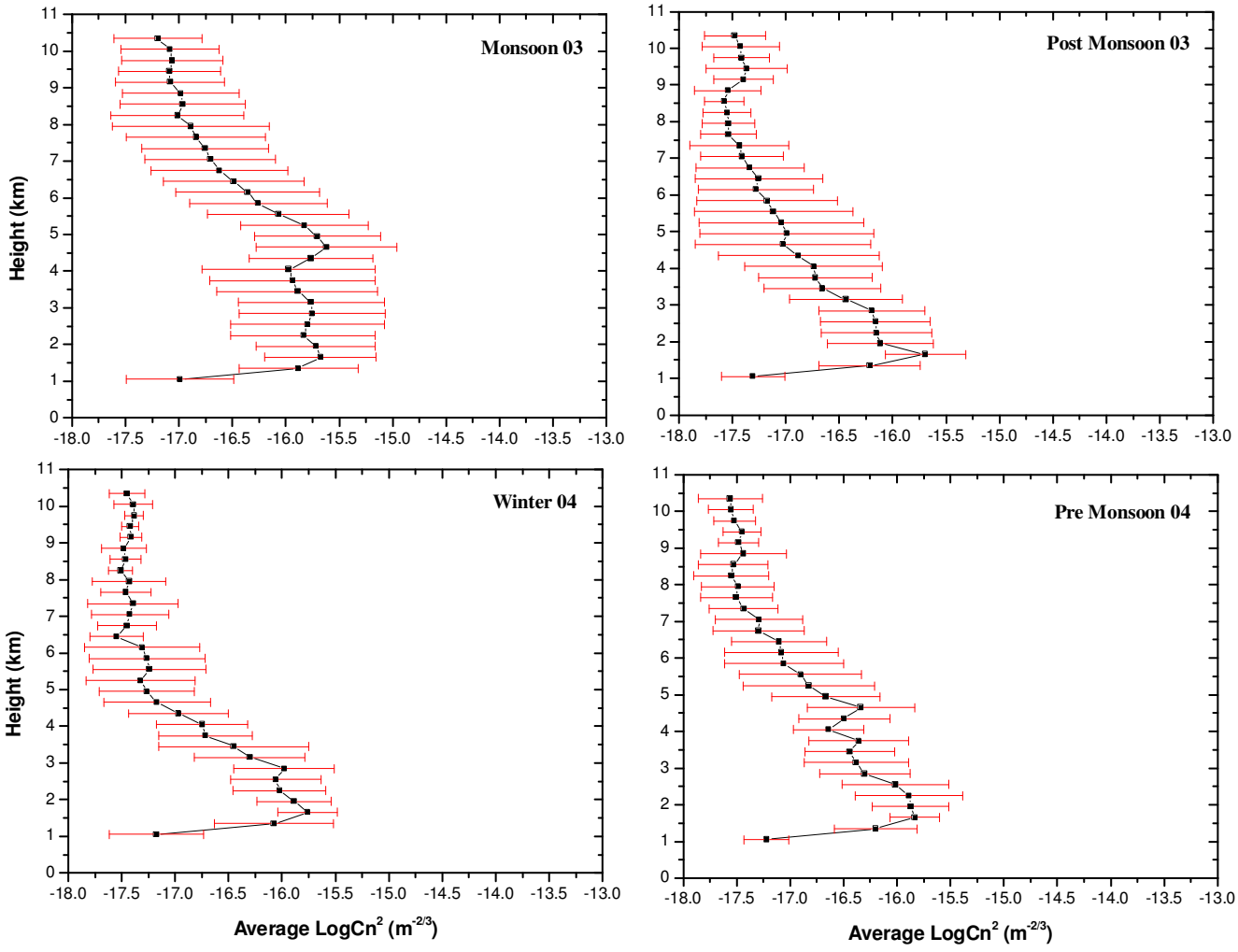

Fig. 2. Seasonal features of C_n^2 with standard deviation, year 2003–2004. Total number of available data points for calculating seasonal mean and standard deviation are 71 (for monsoon 2003, the upper left panel), 76 (for post-monsoon 2003, upper right panel), 54 (for winter 2004, bottom left panel), and 62 (for pre-monsoon 2004, bottom right panel).

3 Results and discussions

3.1 Comparison of C_n^2 derived from wind profiler and RS/RW

Comparison and trend validation of typical C_n^2 values obtained using the WP/RASS data for July 2003, are done with the C_n^2 values calculated from the RS/RW data at 12:00 GMT from the nearby Meteorological station Chikalthana, Aurangabad (19°51′ N, 75°24′ E), because both stations are lying on the leeward side of the western Ghat. In the Fig. 1 the data presented in two panels, each for radiosonde (upper) and wind profiler (lower), is starting at different altitudes as the data available for radiosonde is at 0.6 to about 9.0 km, and wind profiler observations are available in the range gate 1.05–10.35 km. Therefore, we focus the common altitude range 1–9 km for comparing the two results. Moreover, on time axis, the first 3 days in the month of July 2003 do not have the radiosonde observations, therefore rest of the days are considered for the comparative differences in the values of C_n^2. The profiles in Fig. 1 are presented as a function of height above the surface.

Figure 1 depicts that, in the both cases the higher C_n^2 values of the order of magnitude 10^{-14} to $10^{-13}\,\mathrm{m}^{-2/3}$ are observed during active phases of the monsoon in the month of July 2003. There are three active phases each over Pune (days 10, 19–20 and 24–27) and Chikalthana (days 6, 8 and 22–25) during July 2003, showing higher C_n^2 values. However, these three active phases with the C_n^2 values of as much as $10^{-13}\,\mathrm{m}^{-2/3}$ can be clearly identified in the radar observations indicated by the high reflectivity zones in the lower panel of Fig. 1, whereas it is not as clear, except on 6 and 24 July, in the balloon measurements shown in upper panel. This may happen due to the observing differences of balloon

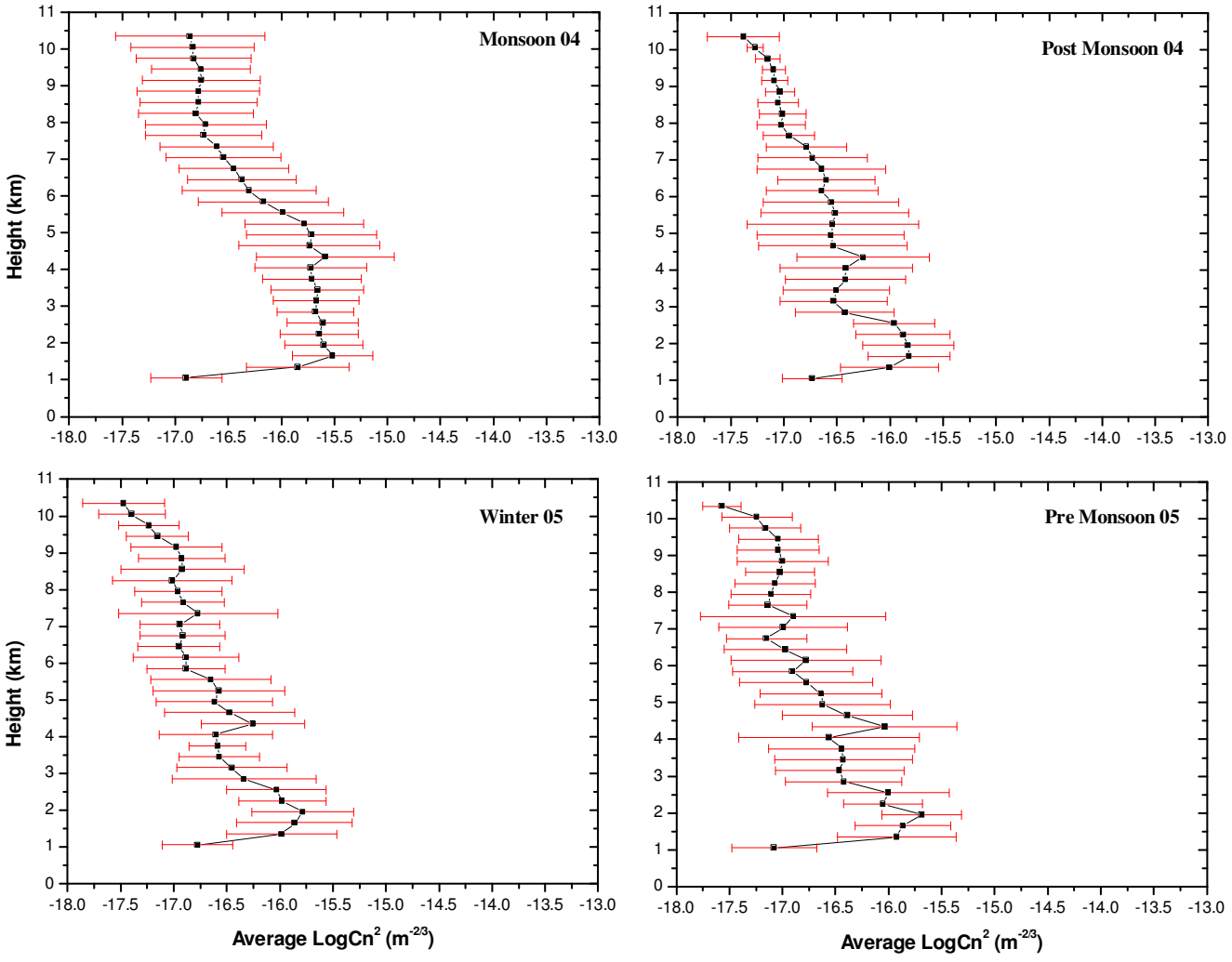

Fig. 3. Seasonal features with standard deviation, year 2004–2005. Total number of available data points for calculating seasonal mean and standard deviation are 77 (for monsoon 2004, the upper left panel), 67 (for post-monsoon 2004, upper right panel), 56 (for winter 2005, bottom left panel), and 73 (for pre-monsoon 2005, bottom right panel).

sounding and the wind profiler (radar gives the volume reflectivity and the balloon a point observation at a particular altitude level). Rainfall recorded in 24 h at Pune and Chikalthana during these active phases is 25–30 mm and 2–11 mm, respectively, given in Indian Daily Weather Report (IDWR-July 2003). Below 1 km, in case of radiosonde data, we see the C_n^2 values of the order of $10^{-13.5}$ to $10^{-13}\,m^{-2/3}$ almost all days in the given month. This is due to the moisture brought through the south westerly winds in the lower troposphere in the month of monsoon. Due to excess humidity present in the atmosphere, we get higher C_n^2 values between 1 and 5 km for both the cases and these values are then decreasing with altitude going down to the $10^{-17.5}$ orders of magnitude. The contours of $\mathrm{Log}C_n^2$ values of -15.5 to $-15\,m^{-2/3}$ are observed in the both data sets, except few patches of $\mathrm{Log}C_n^2$ values of $-16\,m^{-2/3}$ during 8–9 July (radiosonde data) and few regions of high C_n^2 values in active phases as mentioned earlier.

In the case of radiosonde, even after 5 km, the contours of $\mathrm{Log}C_n^2$ display the values of -15.5 and $-15\,m^{-2/3}$ extending up to 9 km, except few days having relatively lower $\mathrm{Log}C_n^2$(days 5, 6, 7 and 8) and on the days 30 and 31 when the observed values are in the range -16.5 to $-17\,m^{-2/3}$ in the height region of 6–9 km. Wind profiler observations show a consistent decrease in the $\mathrm{Log}C_n^2$ values with altitude. At 6–7 km we observe the values between -16.5 and $-16\,m^{-2/3}$ with day to day variations of about -0.5 to $-1.0\,m^{-2/3}$. After 7 km, these $\mathrm{Log}C_n^2$ values decrease from -16.5 to $-17\,m^{-2/3}$, almost in all days of the month. Hence, we conclude that the one-to-one match for each day in this comparison is rather complex to delineate, but the general features exhibit that the C_n^2 ranges from 10^{-13} to

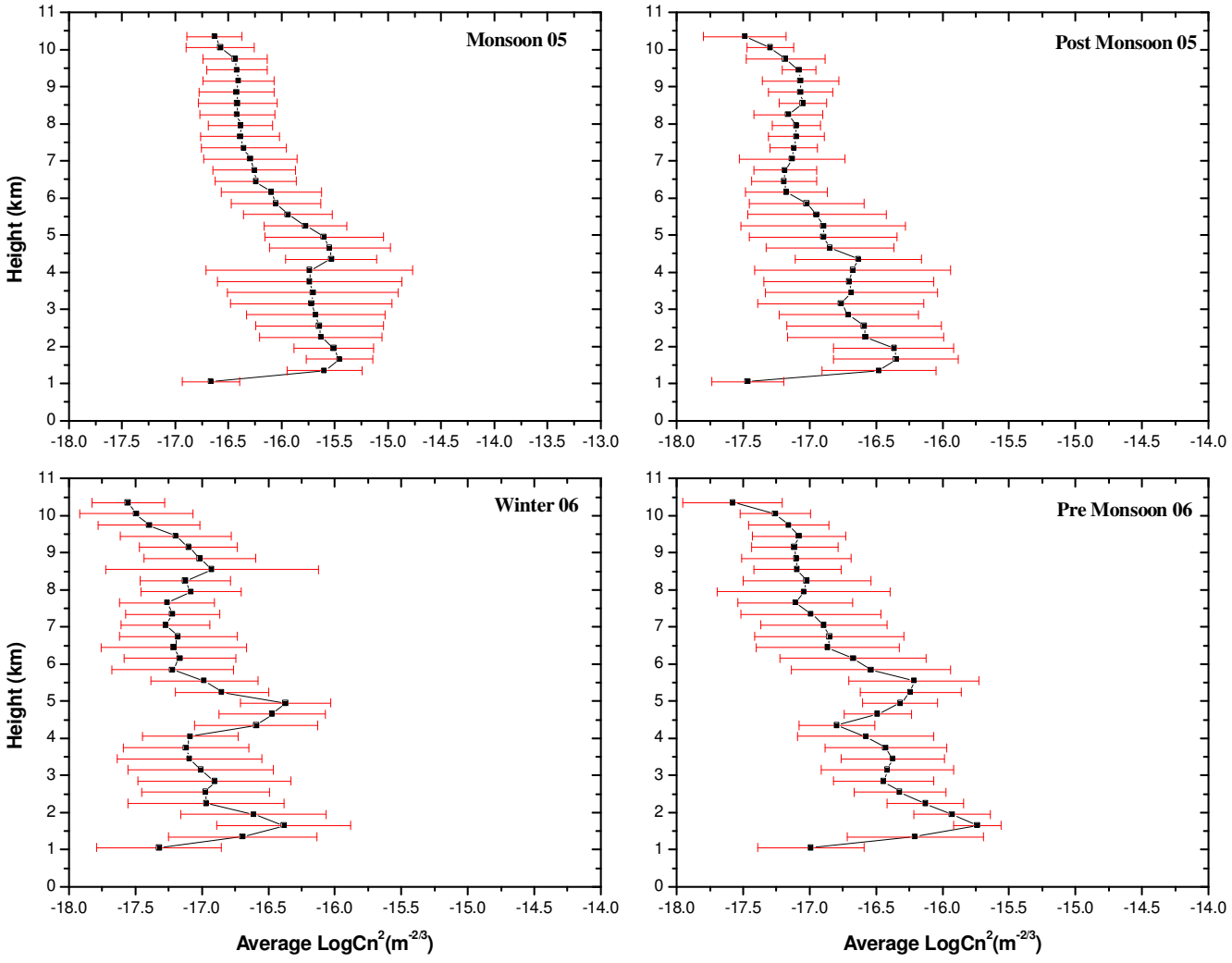

Fig. 4. Seasonal features with standard deviation, year 2005–2006. Total number of available data points for calculating seasonal mean and standard deviation are 95 (for monsoon 2005, the upper left panel), 78 (for post-monsoon 2005, upper right panel), 53 (for winter 2006, bottom left panel), and 57 (for pre-monsoon 2006, bottom right panel).

10^{-18} m$^{-2/3}$ of the order of magnitude and decrease with altitude, in the both cases. The results are comparable in the altitude region 1–5 km, although we observe the differences of about an order of magnitude beyond 5 km within each 2 km. In general, the estimation based on RS/RW data, the Gage et al. (1994) and Van Zandt et al. (1978)'s model, the C_n^2 values are rather higher below 1 km, since during the monsoon season the humidity gradients are suspected to be much larger at the lowest region of the troposphere.

3.2 Seasonal variation of C_n^2

In estimating the turbulence parameter C_n^2, only clear air data from 12:00 GMT is utilized, and the days when precipitation is observed on ground at the radar site, are excluded in all seasons. In Table 2, only monsoon days are given, because in other seasons no precipitation is observed on the site at the time of wind profiler operation.

In Fig. 2, during the monsoon season of the year 2003, we observe bimodal peaks in the C_n^2 values, one near 2 km, located close to the low level jet (LLJ) or top of the boundary layer and another is found at 4–5 km which is at freezing level. This LLJ might be responsible for pumping moisture up to 5 km. Both peaks are due to a high humidity gradient. The peak around 2 km is observed during all seasons. During the monsoon season, high C_n^2 values are seen up to 5 km, which then decrease sharply at higher altitudes. But in other seasons, for example the 2004 winter and premonsoon period above 2 km, C_n^2 values decrease sharply with height. In general, during the monsoon season, the observed C_n^2 values are larger by as much as one order of magnitude than in other seasons. A larger standard deviation is observed during

Table 2. Precipitation days, excluded in studying the turbulence parameters.

Sl. No.	Monsoon season	Months	Date (s)
1.	2003	June	12, 19, 21, 25 and 29
		July	24, 25, 26 and 27
		August	3, 4, 6, 7, 8, 14 and 22
		September	10, 11, 23, 24 and 26
2.	2004	June	2, 3, 6, 9, 13, 14, 15 and 22
		July	NIL (11 days, clear air only)
		August	4, 5, and 11
		September	1, 19, 21, 22, 24 and 25
3.	2005	June	13, 25 and 26
		July	19, 25 and 26
		August	1, 17 and 31
		September	21

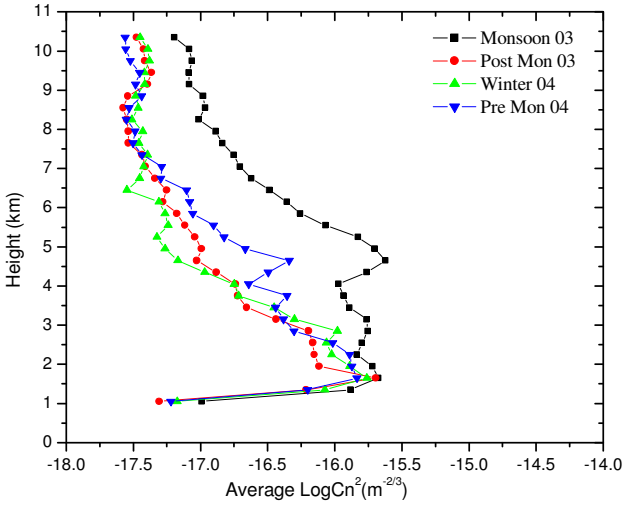

Fig. 5. Height profile of mean LogC_n^2 for different seasons, year 2003–2004.

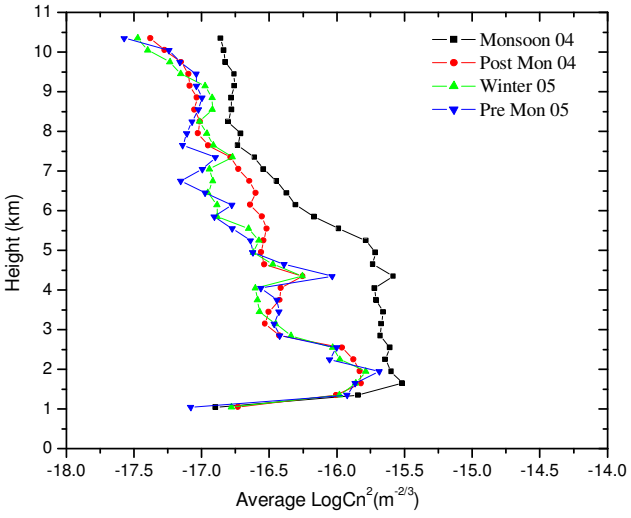

Fig. 6. Height profile of mean LogC_n^2 for different seasons, year 2004–2005.

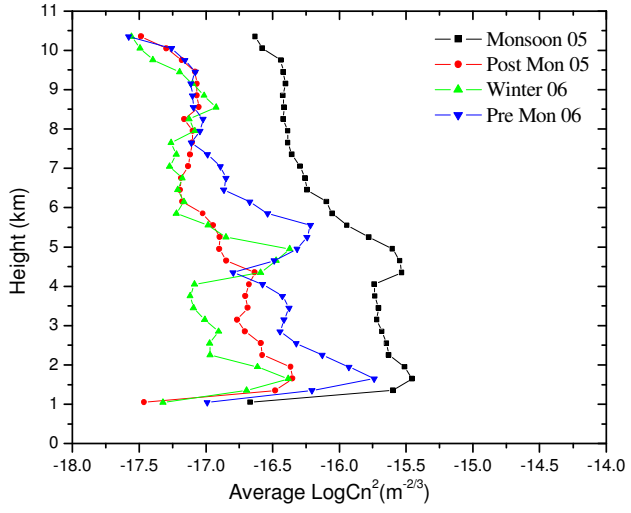

Fig. 7. Height profile of mean LogC_n^2 for different seasons, year 2005–2006.

the monsoon season at all levels up to the height of 10 km, indicating larger humidity fluctuations during the monsoon season. This in turn gives rise to larger gradients in the radio refractive index and hence C_n^2. These fluctuations are seen in other seasons also as found in 2004 winter and pre-monsoon data, but only up to 4–6 km. Above 6 km, fluctuations decrease due to the drastic reduction in the amount of humidity in the atmosphere. Figures 3 and 4 show similar seasonal variations and standard deviations during different years 2004–2006, which indicates that the mean picture during the various seasons of different years remains the same. Since the return signal is determined by humidity gradients, C_n^2 is comparable at lower altitudes for all seasons. The mean values of C_n^2 and ε in the lower troposphere region obtained in the present study are comparable with the values reported by Reddy et al. (2001) (Fig. 3a, b) with 1380 MHz wind profiler located at NARL, Gadanki (13°30′ N, 79°12′ E), India and by Cohn (1995) with the profiler located at, Millstone Hill (42°36′ N, 288°30′ E), Canada. The observed profiles of C_n^2 and ε are in the range from $10^{-17.5}$ to $10^{-13.5}$ m$^{-2/3}$ and 10^{-2} to 10^{-5} m^2 s^{-3}, respectively, for both the latitudes.

The observed/calculated mean profile of C_n^2 as plotted in Figs. 5–7, during the monsoon season for all three years, show that C_n^2 is in the range 10^{-16} to $10^{-15.5}$ m$^{-2/3}$ over the height interval 1–4 km. This is the region where the humidity and its gradient dominate in determining the values of the generalized radio refractive index. It is also the region where the gradient of the potential temperature are almost constant (ref. Eq. 3). Seasonal mean profile of C_n^2 (Fig. 5) shows

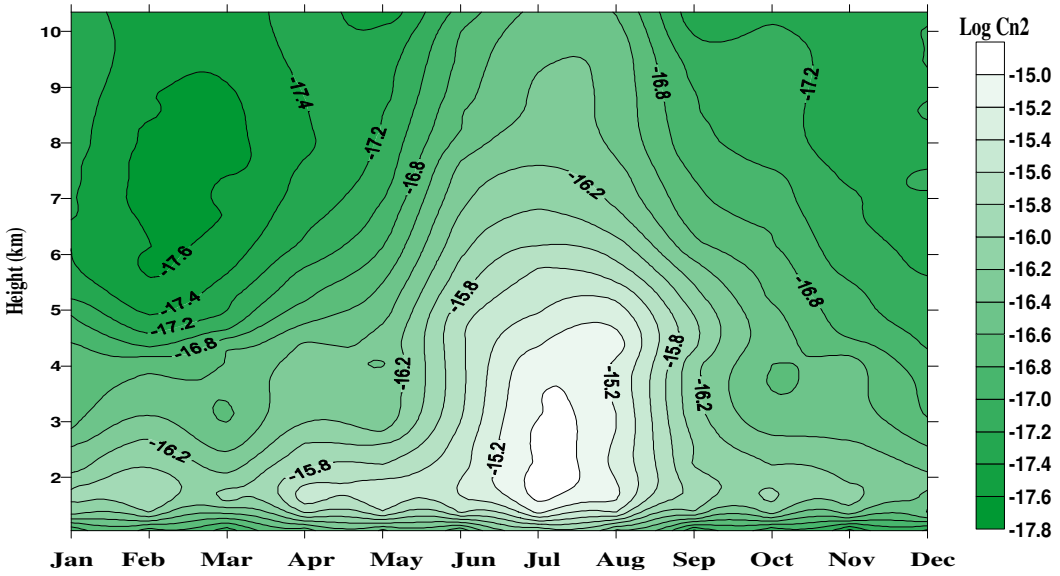

Fig. 8. Contour map for annual features of average LogC_n^2 during 2003–2006. The monthly mean is calculated on daily averaged values 03:00, 06:00, 09:00 and 12:00 GMT at all altitudes between 1 and 10.35 km.

higher values of the order of magnitude 10^{-16} to $10^{-15.5}$ in the altitude range 1–5 km, although in other seasons of the year 2003–2004, the C_n^2 values decrease with altitude and going down from 10^{-16} to $10^{-17.5}$ in the height range 2–10.35 km. The C_n^2 values in the monsoon season of the year 2003–2004 are at least one order higher than those in other seasons, nearly at all altitude levels. In Fig. 6, the observed values of C_n^2 during monsoon season are close to $10^{-15.5}$ in the height range 1–5 km and then decrease with altitude going down to $10^{-16.75}\,\mathrm{m}^{-2/3}$. In comparison to the monsoon seasons of the year 2003 and 2005, the monsoon of 2004 was weaker therefore, particularly in the higher altitudes; we observe the difference of less than one order of magnitude with rest of the seasons. The relatively stronger monsoon of 2005 led the C_n^2 values to be higher around 10^{-16} to $10^{-16.5}\,\mathrm{m}^{-2/3}$ in the altitude range of 7 to 10 km, in contrast to average value of C_n^2 around 10^{-17} for the same altitude region during the monsoon seasons of 2003 and 2004.

Figure 7 indicates that the seasonal mean profile of C_n^2 is nearly same as in the year 2003–2004. The pre-monsoon season of the year 2005–2006 displays larger values than those in winter and post-monsoon, which is likely due to the pre-monsoon thunderstorm activities over Pune. The pre-monsoon curves in Figs. 5–7 do indicate higher average C_n^2 values compared to the cases of winter and post-monsoon periods of the respective years. These higher values appear to have been caused by thunder/thunder showers (8 occurrences in 2004 and 6 each in 2005 and 2006 as reported by IDWR in the corresponding periods). In fact, thunders/thunder showers do occur around the Pune Profiler site even in post-monsoon season also. For example, in post-monsoon period in 2003, three weak and one strong thunderstorm activities were recorded. Corresponding recorded rainfall lying in the range of 1 mm for the weak and 20 mm for the strong case. In 2004 five moderate (rainfall around 6 mm) and two weak (1 mm), and in 2005 three weak (1.6 mm) and one very strong (rainfall in excess of 20 mm) occurrences were recorded. The average C_n^2 curves for the post-monsoon season do reflect these variations by the higher values of C_n^2 observed in the post-monsoon period in 2003 and 2004, compared to the values for 2005, particularly in the altitude region of 1–5 km.

In the winter and pre-monsoon seasons though the temperature gradients remain constant, the humidity decreases significantly and the C_n^2 values decrease in the height range 5–10 km. During the monsoon months of June to September, the C_n^2 values are at least one order of magnitude larger than those during the post-monsoon, winter and pre-monsoon/summer seasons. The increase in C_n^2 that we observe during the monsoon period can be ascribed to increased humidity.

3.3 Annual variability of C_n^2

To study the annual variability of C_n^2, regular observations at 03:00, 06:00, 09:00 and 12:00 GMT of each month, under clear air conditions, are used. The precipitation days as given in Table 2 have been removed. Daily means are further averaged to get monthly means at each height. Monthly means for all three years are averaged to get the respective height profile for January to December.

Figure 8 shows that in the height range of 1.05 to 2 km the mean LogC_n^2 values for the months of January, February, March, April, September, October, November and December are in the range of -15.8 to -16.2 whereas in the months of

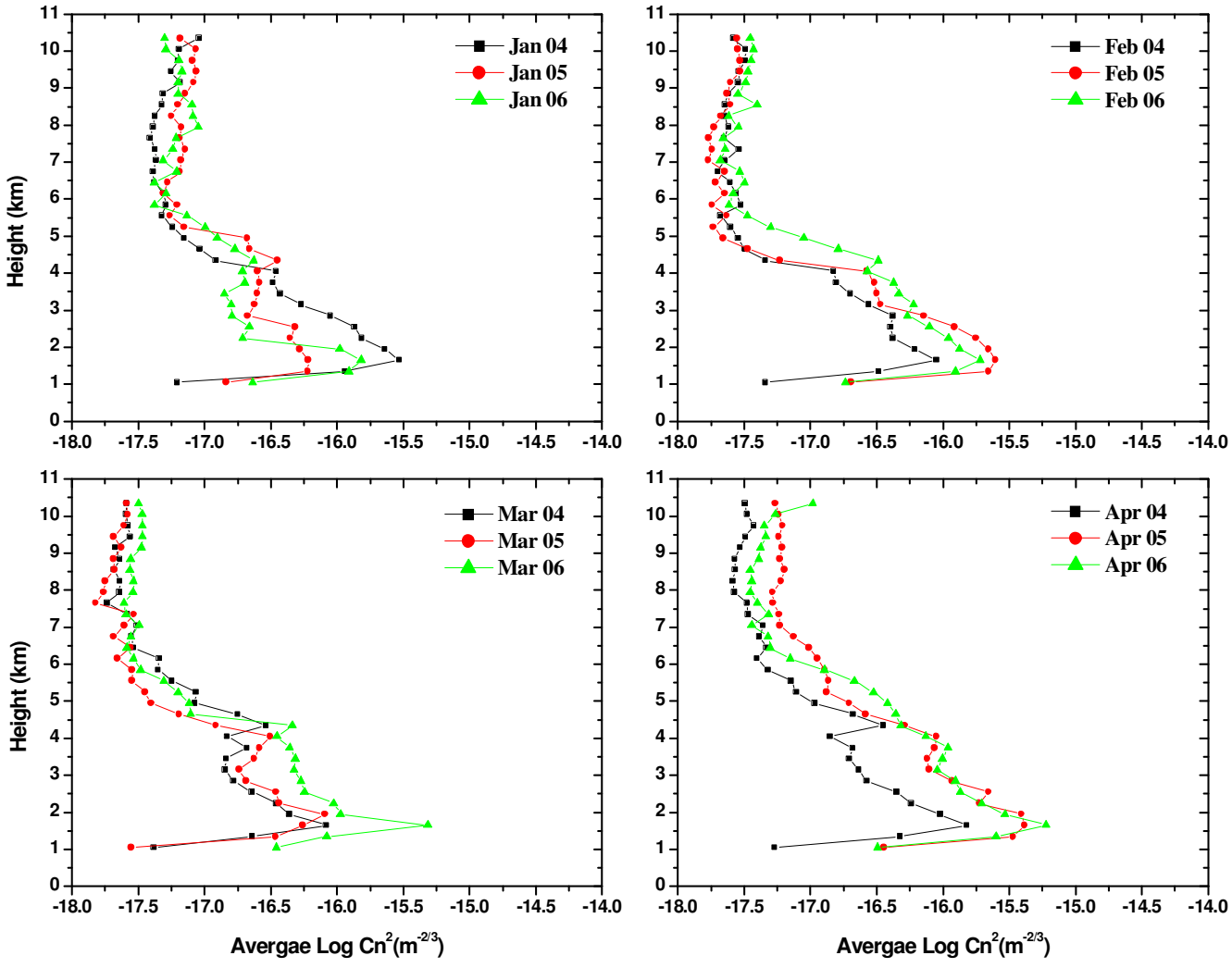

Fig. 9. Height profile of mean LogC_n^2 showing inter-annual features for the months of January, February, March and April.

May, June, July and August the values are higher. Highest C_n^2 values of the order of 10^{-15} are seen in the month of July up to 3.5 km and in the month of June and August slightly lower ($10^{-15.2}\,m^{-2/3}$). In the peak months of monsoon season (June, July and August) higher values of C_n^2 are expected, whereas in the retreating stage of monsoon (September) C_n^2 values are slightly lower of the order of $10^{-15.8}\,m^{-2/3}$. In the months of April, May, October and November the values are relatively lower in the range of 10^{-16} to $10^{-17}\,m^{-2/3}$, though there are some occurrences of thunderstorms in these months, known as pre- and post-monsoon thunder activities. In December, January and February, the driest months of the year, very low values of mean LogC_n^2 in the range of -17 to -18 are observed at heights above 4 km. This is partly because the atmosphere is normally stable with low temperature gradients and so, even if turbulence could be higher, the reflectivity is relatively lower. In general, we see that the larger (at least an order higher as compared with other months) C_n^2 values are observed during June, July and August at all altitudes up to 10 km, indicating that the moisture fluctuations are higher during the monsoon season and extend up to higher altitudes. The contour map in Fig. 8 clearly indicates the higher values of 10^{-16} to 10^{-15} of the order of magnitude are observed during monsoon months and more than an order lower in rest of the months as compared with monsoon months, but consistent decrease with altitude over all months.

3.4 Inter-annual variation of C_n^2

Inter-annual features are also brought out using only clear air data and excluding precipitation spectra for all months of a year. Figures 9, 10 and 11 show the mean picture of C_n^2 for all months over three years of observations. The data is rather short for such a comparison and is only a probable indicative and needs to be confirmed after obtaining data over the

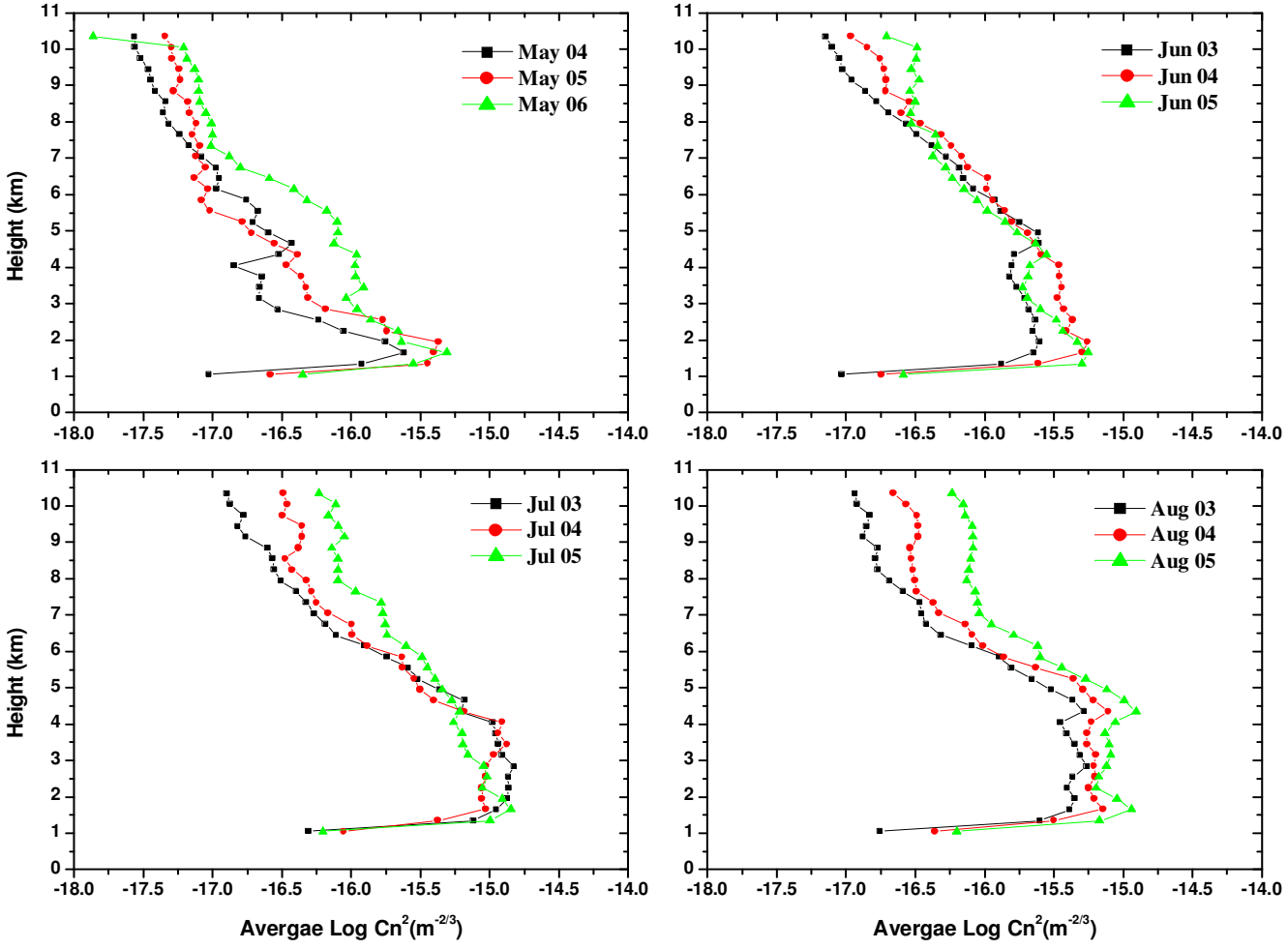

Fig. 10. Height profile of mean LogC_n^2 showing inter-annual features for the months of May, June, July and August.

number of years. The radar was operational since June 2003 and therefore, January–May during the period 2004–2006 and June–December during the period 2003–2005 are taken to show the inter-annual variability. In the months January–April (Fig. 9), March (Fig. 10), and October–December (Fig. 11), we notice a larger range of C_n^2 values, $10^{-17.3}$ to $10^{-15.25}\,m^{-2/3}$ in the altitude 1.65–4 km, however the observed year-to-year variability at a particular altitude level is very less, except few cases (4 January, 6 March, 5–6 April, 3 November, 3 December) where the variations are significant. But these variations from one year to the other in a particular month are always much less than an order of magnitude, almost at all the range bins and mean picture remains the same. Moreover, steeper gradients of C_n^2 values are seen in the height range 1.35–4 km in all months of a year, other than monsoon months (June–September). In the monsoon months during the three years, the observed values of C_n^2 are in the range $10^{-14.8}$ to $10^{-16.2}\,m^{-2/3}$ in the altitude 1.35–4.35 km and the gradients are also less (almost constant) as compared to the rest of the months. Now, it is interesting to see that the gradients reverse in the height range from about 4.5–10.35 km and the larger gradients occur in monsoon months than the other months during the three years of observation. This is because the monsoon brings adequate amount of moisture in the tropical lower troposphere, but the humidity drastically reduces after about 6 km.

Above 4.5 km, the observed C_n^2 values in monsoon months are in the range $10^{-15.25}$ to $10^{-17.25}\,m^{-2/3}$, whereas in other months these are in the range $10^{-16.25}$ to $10^{-17.8}\,m^{-2/3}$. At higher altitudes (4–10.35 km), the observed year-to-year variations during all months are not significant and show the similar pattern, except small year-to-year fluctuation in the months of May 2006, July–August 2005 and November 2004. In the month of March 2006, mean C_n^2 values are relatively lager than the other years because the abnormal rainfall was recorded in this month (10 mm). Similarly, the relatively higher values of mean C_n^2 up to 6 km are observed in April 2005 and 2006, since there were abnormal rains (9.3 mm) in April 2005 and rather cloudy skies with relatively high humidity up to higher altitudes in April 2006. In the month

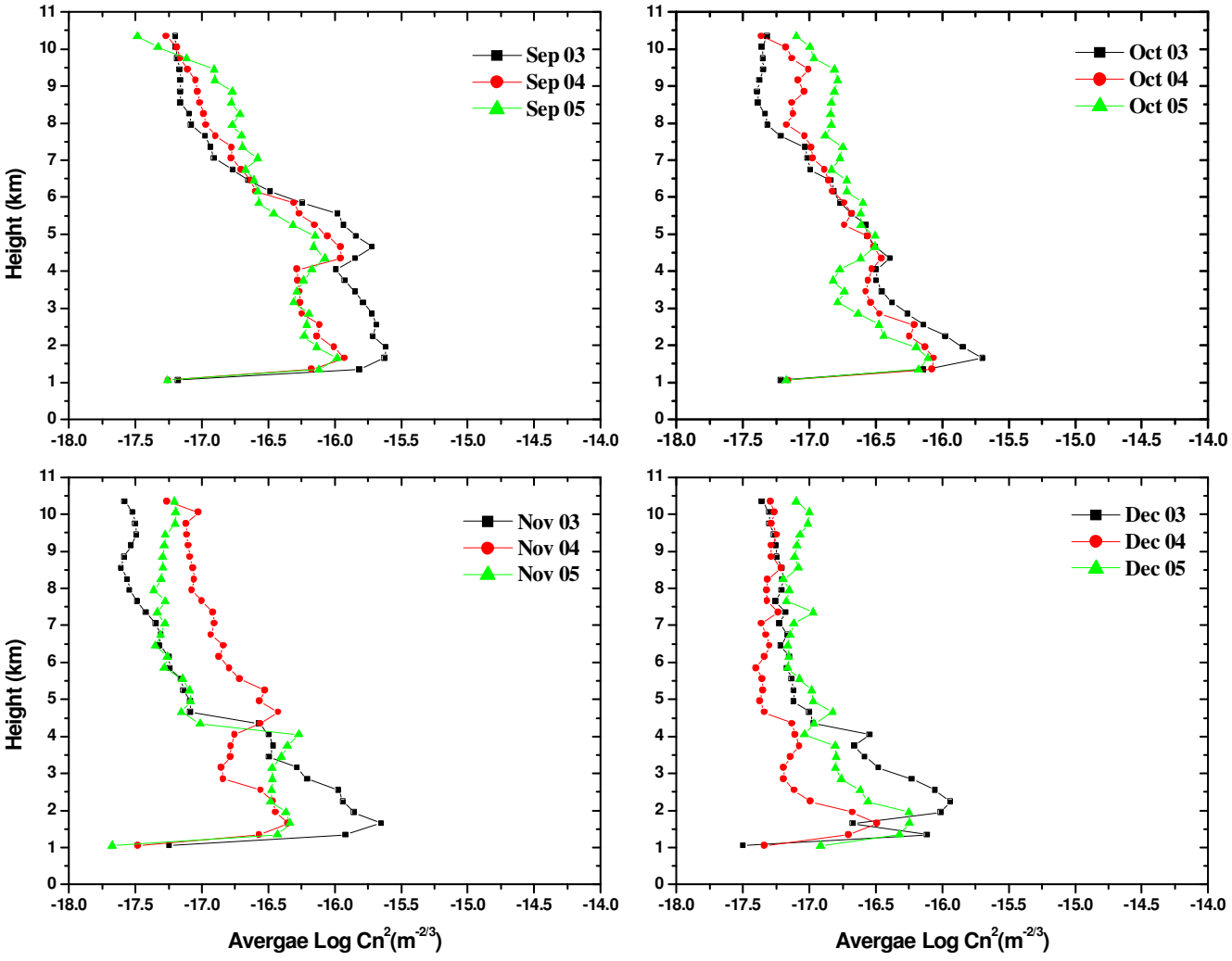

Fig. 11. Height profile of mean LogC_n^2 showing inter-annual features for the months of September, October, November and December.

of May 2006, mean C_n^2 values are much higher relative to 2004 and 2005 because of the heavy pre-monsoon showers at observation site. Corresponding rainfall recorded in May 2004, 2005 and 2006 is 9.15 mm, 10.66 mm and 18.7 mm, respectively. November 2004 recorded the abnormal rainfall of 2.8 mm. In the monsoon months (June–September), the mean C_n^2 values show typical pattern of bimodal peaks, one near 2 km and another about 4 km, and higher values of C_n^2 are observed up to 4–5 km, which continuously decreases up to 10 km. Hence, as discussed above, the year-to-year variability in a particular month is always much lesser than an order of magnitude and beyond 6 km altitude, very small fluctuations are observed in all months except few cases.

3.5 Seasonal variation of eddy dissipation rate (ε)

We present only one year of data in calculating the energy dissipation rates. More years of the data still need to be examined for the various quality control checks in all three beams, so that the consistency in the data may be maintained up to 10.35 km. In the data presented here for the year 2004–2005, ε estimates are reliable up to 6 km and thereafter random fluctuations are observed from 1 range gate to the other within 300 m of spatial resolution, right up to 10.35 km. Figure 12 shows the energy dissipation rates with higher standard deviation in the height range 4–8 km than below 4 km where the fluctuations are smaller. In the monsoon months the fluctuations are gradually increasing with height, whereas in other seasons the fluctuations in the altitude 1–3.5 km are lower than those observed above 3.5 km. Since the signal strength is drastically reduced above 6 km, the observed fluctuations at higher altitudes are therefore larger, and the estimates of ε above 6 km are not quite reliable. The observed values of ε in all seasons (except slightly higher in pre-monsoon and monsoon) as shown in Fig. 13 range from 10^{-3} to $10^{-3.75}$ m^2 s^{-3} in the lower 3 km and decreasing with altitude.

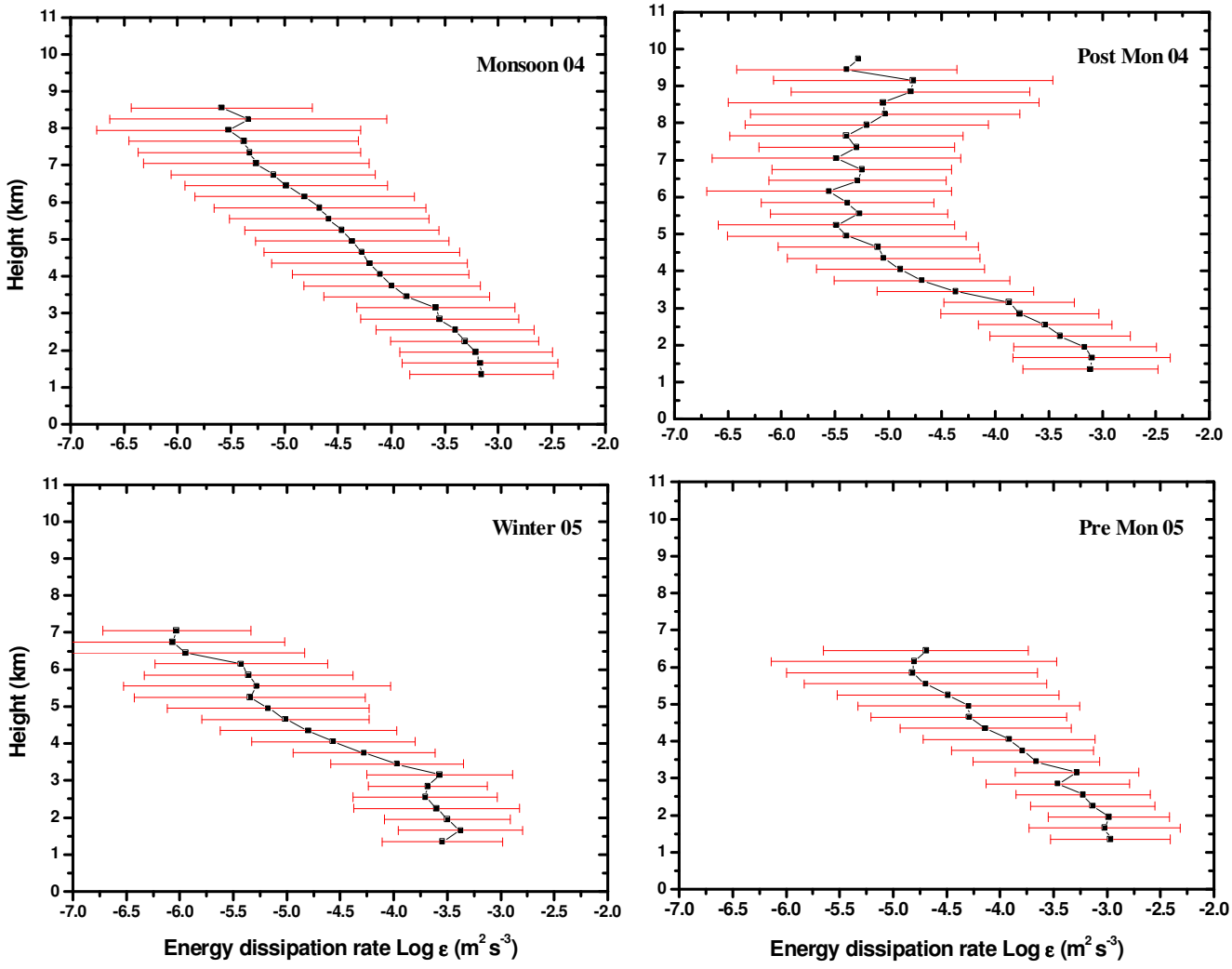

Fig. 12. Energy dissipation rates with standard deviation, 2004–2005. Total number of available data points for calculating seasonal mean and standard deviation of ε are, 82 (for monsoon 2004, the upper left panel), 66 (for post-monsoon 2004, upper right panel), 53 (for winter 2005, bottom left panel), and 87 (for pre-monsoon 2005, bottom right panel).

In pre-monsoons and monsoon seasons, large values of ε, 10^{-3} to $10^{-4.75}$ m^2 s^{-3}, are observed in the height range 1–6 km, whereas largest values, 10^{-3} to $10^{-3.5}$ m^2 s^{-3} are confined in the altitude range 1–3 km. Convective activities and low level jet aid in pumping more moisture in to the free atmosphere, and strong wind shear in the LLJ boundaries further enhances the turbulence in the atmosphere. Post-monsoon and winter seasons are found to have ε values of 10^{-3} to $10^{-5.7}$ in the altitude 1–6 km, though ε in the lower 3 km is closer to that in monsoon. Pre-monsoon and monsoon months show gradual decrease with altitude in ε values, as compared with the post-monsoon and winter months, and above 6 km a random variation is seen in all seasons as mentioned above. Also, the values of ε in the lower troposphere, particularly in the height region 1–6 km, are comparable with the values reported by Cohn (1995) and Hocking and Mu (1997). It is evident that, the estimated ε values are in the range of 10^{-3}–10^{-6} m^2 s^{-3}. The presented high resolution observations at 404 MHz are first of its kind from tropical India, revealing the seasonal pattern during a year and will be investigated in detail after archiving the data for number of years.

4 Conclusions

The refractive index structure parameter (C_n^2) is one of the basic variables of atmospheric turbulence which can be determined using the radar measurements of the received echo intensity (viz. VanZandt et al., 1978; Hocking et al., 1989). The radar echo arises due to refractive index irregularities, associated with turbulence on a scale equal to half of the radar

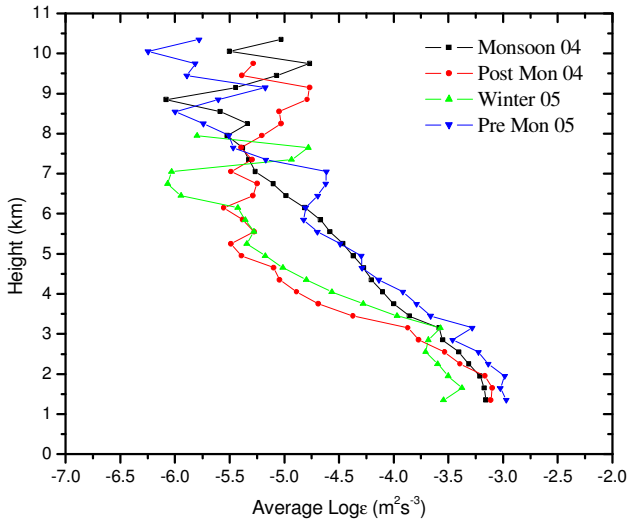

Fig. 13. Height profile of mean energy dissipation rates during different seasons, 2004–2005.

wavelength ($\lambda/2$). For example, wind profiler at Pune operates at 404 MHz and half of its wavelength is about 0.37 m and thus, the radar samples the refractive index irregularities of this scale. In the present article, an attempt is made to understand the seasonal, annual and inter-annual variability in C_n^2 with the seasonal features of ε, in the altitude of 1–10.35 km. For the first time, observations taken with the 404 MHz wind profiler at Pune provided a unique opportunity to study the turbulence parameters over the tropical station, and this study will help in understanding the lower atmospheric dynamics in the tropics. Sarkar et al. (1985) have calculated values of C_n^2 up to 5 km only, and they show an exponentially decreasing trend from 1–5 km over all Indian regions and for all seasons. We observe bimodal peaks during the monsoon season and one peak in other seasons. In the present study, an attempt has been made to examine the seasonal, annual and inter-annual features of the refractive index structure parameter C_n^2.

The observed mean values for C_n^2 are in the range from $10^{-17.5}$ to $10^{-13}\,m^{-2/3}$. In the monsoon season the observed average values, during the span of three years, are 10^{-16} to $10^{-15.5}\,m^{-2/3}$ in the lower troposphere. The values decrease with height, but at a slightly higher rate than during other seasons, at all levels up to 10 km. In the post monsoon, winter and summer seasons, C_n^2 values are from 10^{-17} to $10^{-16}\,m^{-2/3}$ in the height range 1–4 km and then decreases to $10^{-17.8}$ at higher altitudes. The highest observed values are from $10^{-13.5}$ to 10^{-13} during situations with rain. Since previous observations of C_n^2 using radars have been carried out at mid and high latitudes (Gage et al., 1978, 1990; Smith et al., 1983; Nastrom et al., 1986; Hocking et al., 1989), only a few measurements are available at tropical and low latitude regions (Sato and Woodman, 1982; Tsuda et al., 1985; Rao et al., 1997, 2001a, b; Ghosh et al., 2001). Therefore, this study contributes to the real time observations for understanding the lower tropospheric dynamics in the tropics.

Seasonal features of the energy dissipation rate (ε) are also studied. Doppler spectral widths of the received radar back scattered signal are related to the turbulence velocity field. The observed spectral width arise due to contributions from atmospheric turbulence as well as non turbulent effects such as beam broadening and shear broadening (Fukao et al., 1994; Nastrom, 1997). These contaminations are removed to obtain a correct estimate of ε. The observed average values of $\log \varepsilon$ are in the range -6.4 to $-3.0\,m^2\,s^{-3}$, and it continuously decreases with heights. Relatively higher dissipations rates are observed during the pre-monsoon and monsoon seasons.

Acknowledgements. The authors express their sincere gratitude towards the technical staff of India Meteorological Department at Pashan Branch, Pune for their co-operation during radar observations and the technical team of SAMEER Mumbai specifically to Kiran More looking after the radar system at site for uninterrupted operation and maintenance. Thanks are due to J. R. Kulkarni for his valuable suggestions and critical comments.

Topical Editor U.-P. Hoppe thanks two anonymous referees for their help in evaluating this paper.

References

Bakker, A.: MIT Lecture notes on Kolmogorov Theory, 2002.

Balsley, B. B. and Gage, K. S.: On the use of radars for operational profiling, B. Am. Meteorol. Soc., 63, 1009–1018, 1982.

Cohn, S. A.: Radar measurement of turbulent eddy dissipation rate in the troposphere a comparison of techniques, J. Atmos. Ocean. Technol., 12, 85–95, 1995.

Doviak, R. J. and Zrnic, D. S.: Doppler radar and Weather Observations, Academic Press, Orlando, FL, 468, 1993.

Ecklund, W. L., Carter, D. A., and Balsley, B. B.: A UHF wind profiler for the boundary layer: Brief description and initial results, J. Atmos. Ocean. Technol., 5, 432–441, 1988.

Frisch, A. S. and Clifford, S. F.: Study of Convection Capped by a Stable Layer Using Doppler Radar and Acoustic Echo Sounders, J. Atmos. Sci., 31(6), 1622–1628, 1974.

Fukao, S., Yamanaka, M. D., Naoki, A. O., Hocking, W. K., Sato, T., Yamamoto, M., Nakamura, T., Tsuda, T., and Kato, S.: Seasonal variability of vertical eddy diffusivity in the middle atmosphere 1. Three-year observations by the middle and upper atmosphere radar, J. Geophys. Res., 99, 18 973–18 987, 1994.

Gage, K. S.: Radar observations of the free atmosphere: structure and dynamics, edited by: Atlas, D., Radar in Meteorology, Am. Meteorol. Soc., Boston, 534–565, 1990.

Gage, K. S. and Balsley, B. B.: Doppler radar probing of clear atmosphere, B. Am. Meteorol. Soc., 59, 1074–1093, 1978.

Gage, K. S., Williams, C. R., and Ecklund, W. L.: UHF wind profilers: a new tool for diagnosing tropical convective cloud systems, B. Am. Meteorol. Soc., 75, 2289–2294, 1994.

Ghosh, A. K., Sivakumar, V., Kishore Kumar, K., and Jain, A. R.: VHF Radar Observations of Atmospheric Winds, associated

shears and C_n^2 at a tropical location: Interdependence and Seasonal Pattern, Ann. Geophys., 19, 965–973, 2001, http://www.ann-geophys.net/19/965/2001/.

Gossard, E. E. and Strauch, R. G.: Radar observation of clear air and clouds, Elsevier science publishers (UK), 280 p., 1983.

Gossard, E. E., Wolfe, D. E., Moran, K. P., Paulus, R. A., Anderson, K. D., and Rogers, L. T.: Measurement of Clear-Air Gradients and Turbulence properties with Radar wind profilers, J. Atmos. Ocean. Technol., 15, 321–342, 1998.

Hocking, W. K.: On the extraction of atmospheric turbulence parameters from radar backscatter Doppler spectra-I, Theory, J. Atmos. Terr. Phys., 45, 89–102, 1983.

Hocking, W. K.: Measurement of turbulent energy dissipation rates in the middle atmosphere by radar techniques, Radio Sci., 20, 1403–1422, 1985.

Hocking, W. K., Lawry, K., and Neudegg, D.: Radar measurement of atmospheric turbulence intensities by C_n^2 and spectral width method. Middle atmosphere program hand book, 27, 443–446, SCOSTEP secretariat, Univ. Illinois, 1989.

Hocking, W. K.: An assessment of the capabilities and limitations of radar in measurements of upper atmosphere turbulence, Adv. Space Res., 17(11), 37–47, 1996.

Hocking, W. K. and Mu, K. L.: Upper and middle tropospheric kinetic energy dissipation rates from measurements of C_n^2 – review of theories, in-situ investigations, and experimental studies using Backland Park atmospheric radar in Australia, J. Atmos. Terr. Phys., 59(14), 1779–1803, 1997.

Jain, A. R., Jaya Rao, Y., Rao, P. B., Anandan, V. K., Damle, S. H., Balamuralidhar, P., Kulakerni, A., and Viswanathan, G.: Indian MST radar, 2. First scientific results in ST mode, Radio Sci., 30, 1139–1158, 1995.

Joshi, R. R., Narendra Singh, Deshpande, S. M., Damle, S. H., and Pant, G. B.: UHF wind profiler observations of monsoon low level jet over Pune, Indian J. Radio Space Phys., 35, 349–359, 2006.

Nastrom, G. D., Gage, K. S., and Ecklund, W. L.: Variability of turbulence, 4-20km, in Colorado and Alaska from MST radar observations, J. Geophys. Res., 91, 6722–6734, 1986.

Nastrom, G. D.: Doppler radar spectral width broadening due to beamwidth and wind shear, Ann. Geophys., 15, 786–796, 1997, http://www.ann-geophys.net/15/786/1997/.

Pant, G. B., Joshi, R. R., Damle, S. H., Deshpande, S. M., Singh, N., Vashistha, R. D., Neekhara, P., Chande, J. V., Kulkarni, A. A., and Pillai, J. S.: Wind profiler and Radio Acoustic Sounding System at IMD, Pune: Some preliminary results, Current Sci., 88, 761–769, 2005.

Ralph, M. F., Neiman, P. J., Van De Kamp, D. W., and Low, D. C.: Using spectral moment data from NOAA 404 MHz radar wind profiler to observed precipitation, B. Am. Meteorol. Soc., 76, 1717–1739, 1995.

Rao, D. N., Kishore, P., Rao, T. N., Vijaya Bhaskara Rao, S., Reddy, K. K., Yarraiah, M., and Hareesh, M.: Studies on refractivity structure constant, eddy dissipation rate and momentum flux at a tropical latitude, Radio Sci., 32, 1375–1389, 1997.

Rao, T. N., Rao, D. N., Mohan, K., and Raghavan, S.: Classification of tropical precipitating systems and associated Z-R relationships, J. Geophys. Res., 106, 17 699–17 711, 2001a.

Rao, D. N., Ratnam, M. V., Narayan Rao, T., and Vijaya Bhaskara Rao, S.: Seasonal variation of vertical eddy diffusivity in the troposphere, lower tratosphere and mesosphere over a tropical station, Ann. Geophys., 19, 975–984, 2001b, http://www.ann-geophys.net/19/975/2001/.

Reddy Kalapureddy, M. C., Kumar, K. K., Shivakumar, V., Ghosh, A. K., Jain, A. R., and Reddy, K. K.: Diurnal and seasonal variability of TKE dissipation rate in the ABL over a tropical station using UHF wind profiler, J. Atmos. Solar Terr. Phys., 69, 419–430, 2007.

Rogers, R. R., Ecklund, W. L., Carter, D. A., Gage, K. S., and Ethier, S. A.: Research Applications of a boundary-layer wind profiler, B. Am. Meteorol. Soc., 74, 567–580, 1993.

Sarkar, S. K., Pasricha, P. K., Dutta, H. N., Reddy, B. M., and Kulshrestha, S. M.: Atlas of Tropospheric Radio Propagation Parameters over the Indian subcontinent, published by National Physical Laboratory, Delhi, p. 200–239, 1985.

Satheesan, K. and Krishna Murthy, B. V.: Turbulence parameters in the tropical troposphere and lower stratosphere, J. Geophys. Res., 107(D1), 4002, doi:10.1029/2000JD000146, 2002.

Sato, T. and Woodman, R. F.: Fine altitude resolution observations of stratospheric turbulent layers by the Arecibo 430-MHz radar, J. Atmos. Sci., 39, 2546–2552,1982.

Smith, S. A., Romick, G. J., and Jayaweera, K.: Poker Flat MST observations of shear-induced turbulence, J. Geophys. Res., 88, 5265–5271, 1983.

Tatarskii, V.: The effect of turbulent atmosphere on wave propagation. National technical information series; Springfield, p. 74–76, 1971.

Tsuda, T., Hirose, K., Kato, S., and Sulzer, M. P.: Some finding on correlation between the stratospheric echo power and the wind shear observed by the Aericibo UHF radar, Radio Sci., 20, 1503–1508, 1985.

Van Zandt, T. E., Green, J. L., Gage, K. S., and Clark, W. L.: Vertical profiles of reflectivity turbulence structure constant: Comparison of observations by the Sunset Radar with a new theoretical model, Radio Sci., 13, 819–829, 1978.

Weinstock, J.: On the theory of turbulence in the buoyancy subrange of stably stratified flows, J. Atmos. Sci., 35, 634–649, 1978.

White, A. B., Lataitis, R. J., and Lawrence, R. S.: Space and time filtering of remotely sensed velocity turbulence, J. Atmos. Ocean. Technol., 16, 1967–1972, 1999.

Williams, C. R., Ecklund, W. L., and Gage, K. S.: Classification of precipitating clouds in the Tropics using 915-MHz wind profilers, J. Atmos. Ocean. Technol., 12, 996–1012, 1995.

Zink, F., Vincent, R. A., Murphy E., and Cote, O.: Comparison of radar and in situ measurements of atmospheric turbulence, J. Geophys. Res., 109, D11108, doi:10.1029/2003JD003991, 2004.